PCCP

Accepted Manuscript

Chemical Activity of Oxygen Vacancies on Ceria: A combined Experimental and Theoretical Study on CeO2 (111)

Chengwu Yang,[†] Li-Li Yin,[‡] Fabian Bebensee,[†] Maria Buchholz,[†] Hikmet Sezen,[†] Stefan Heissler,[†] Jun Chen[†], Alexei Nefedov,[†] Hicham Idriss,[§] Xue-Qing Gong,*,[‡] and Christof Wöll*,[†]

[†]Institut für Funktionelle Grenzflächen, Karlsruher Institut für Technologie, 76021 Karlsruhe, Germany

[‡]Key Laboratory for Advanced Materials, Centre for Computational Chemistry and Research Institute of Industrial Catalysis, East China University of Science and Technology, Shanghai 200237, P.R. China

[§]Saudi Basic Industries Corporation (SABIC), CRI at KAUST, Thuwal, P.O Box 4545-4700, Saudi Arabia

ABSTRACT: The chemical activity of oxygen vacancies on well-defined, single-crystal $CeO_2(111)$-surfaces is investigated using CO as a probe molecule. Since no previous measurements are available, the assignment of the CO ν_1 stretch frequency as determined by IR-spectroscopy for the stoichiometric and defective surfaces are aided by ab-initio electronic structure calculations using density functional theory (DFT).
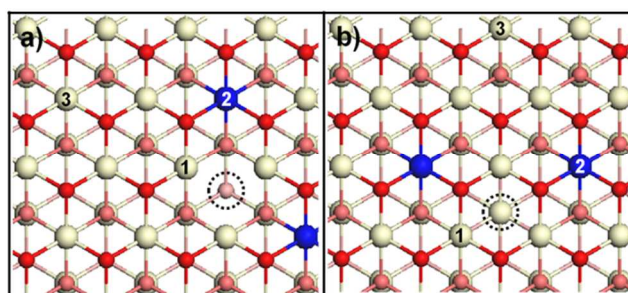
Fig.1. Ball-and-stick model of the $CeO_2(111)$ surface (top view) with (a) top- or (b) subsurface oxygen vacancy (V_o). The position of the vacancy is indicated by the dashed circle. Color: red – top surface oxygen, light red – subsurface oxygen, white – Ce^{4+}, blue – Ce^{3+}.

Ceria, one of the most easily reducible materials,[1] provides the basis for numerous applications ranging from heterogeneous catalysis (vehicle emission control, ethanol steam reforming,[2] water gas shift reactions[3-5]) over solar thermal hydrogen production from water[6-8] and to the generation of CO from CO_2.[9] In all cases, the oxidation reduction cycle (Ce^{4+}/Ce^{3+} cations – and the associated oxygen vacancies) is the most determining factor. The importance of this material has triggered numerous experimental and theoretical studies, in particular aiming at elucidating the properties of oxygen vacancies. Earlier pictures proposing the two electrons left behind by removing an oxygen atom from the surface to be localized at the surrounding cations (i.e., presence of two Ce^{3+} ions adjacent to the defect, see the Ce cations labeled 1 in Fig. 1) had to be revised later[10] and recent theoretical work has revealed that the remaining electrons are actually localized at some distance away from the vacancy.[11-15] Though it is intuitive to believe that the density of oxygen vacancies may affect the chemical activity of ceria, direct experimental evidence is lacking and even the determination of O-vacancy densities represents a major experimental challenge. The most frequently used approach to determine the concentration of this active site crucial for all redox reactions occurring on this surface is to use carbon monoxide (CO) as a probe molecule and to deduce the nature of the cations it binds to from the frequency of the CO stretch vibration (ν_1). For ceria powder particles, this frequency can be determined conveniently from Infrared (IR) spectroscopy.[16-25] Typically, the CO stretch frequency shows

substantial variations upon changes in the charge state of the metal ion the CO is bound to. In the case of Cu ions, for example, the difference in stretch frequency between CO bound to Cu^{2+} and Cu^+ amounts to about 70 cm^{-1}.[26] Although a large set of data exists for CO adsorbed on ceria powders, the extent of this shift for Ce-cations is still being discussed quite controversially.[27] For a reliable identification of the shifts urgently reference data for ceria single crystal surfaces are needed.[28]

EXPERIMENTAL

The IRRAS measurements were conducted in an UHV apparatus combining a state-of-the-art FTIR spectrometer (Bruker Vertex 80v) with a multi-chamber UHV system (Prevac).[29] The $CeO_2(111)$ single crystal (SurfaceNet) surface was prepared by repeated cycles of sputtering with 1 keV Ar^+ and annealing at 800 K for 15 min in an O_2 atmosphere of 1×10^{-5} mbar for forming a stoichiometric surface, or alternately without O_2 to create a reduced one. Exposure to CO at sample temperatures typically below 75 K was achieved by backfilling the IR chamber up to 10^{-9} mbar. The base pressure during acquisition of IR spectra was $\sim8\times10^{-11}$ mbar.
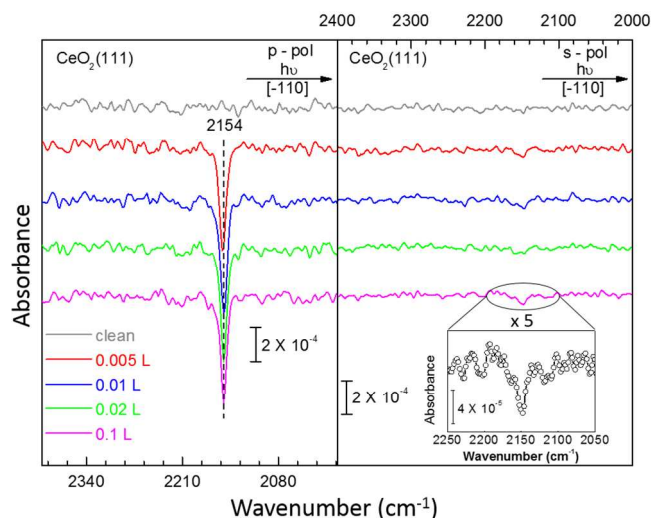
Fig. 2. Experimental IRRA spectra of different doses of CO at 68 K on stoichiometric CeO_2 (111) at a grazing incidence angle of 80° with (left) *p*- and (right) *s*-polarized light incident along [-110]. The inset shows a blow-up of the spectral region marked with an ellipse.

IR spectra were recorded with both s- and p-polarized light incident along the [-110] and [-211] crystallographic directions. For further details see the SI section.

Computational Methods

Spin-polarized density functional theory calculations corrected by on-site Coulomb interaction (DFT+U) have been performed by using the VASP package.[30,31] The Perdew-Burke-Ernzerhof (PBE) functional,[32,33] based on the generalized gradient approximation (GGA), was employed to evaluate the non-local exchange-correlation energy. The plane wave energy cutoff was 400 eV, and the core-electron interactions were described by the projector-augmented wave method (PAW),[34,35] with the Ce (4f, 5s, 5p, 5d, 6s), O (2s, 2p) and C (2s, 2p) electrons treated as valence electrons.[36,37] For further details see the SI.

RESULTS

In the present study, we first determined the stretch frequency of CO adsorbed on a fully-oxidized, single crystalline CeO_2(111) surface ("stoichiometric surface") using infrared reflection absorption spectroscopy (IRRAS). The single sharp band seen in Fig.2 indicates that ν_1 for CO adsorbed on the fully oxidized CeO_2(111) surface amounts to 2154 cm^{-1}, thus allowing to correct previous assignments made on the basis of powder data (see Table S1 in the SI).

It should be noted that the peak is negative, in accordance with IR-data data recorded for CO adsorbed on other oxide surfaces.[38] Only a very weak, also negative, feature was observed for s-polarized light (see SI for data with different incidence geometries).

In a next step, we deliberately introduced oxygen vacancies on the CeO_2(111) surface ("reduced surface"). For a defect density of around 9% (as determined form XPS, see SI), the data shown in Fig. 3 clearly reveal the presence of a new species at 2163 cm^{-1}. IR-spectra recorded at different temperatures (see Fig. S5) allow determining the binding energy of the two different CO species - a quantitative analysis yields 0.27 eV and 0.31 eV, for the ideal and the defective site, re-

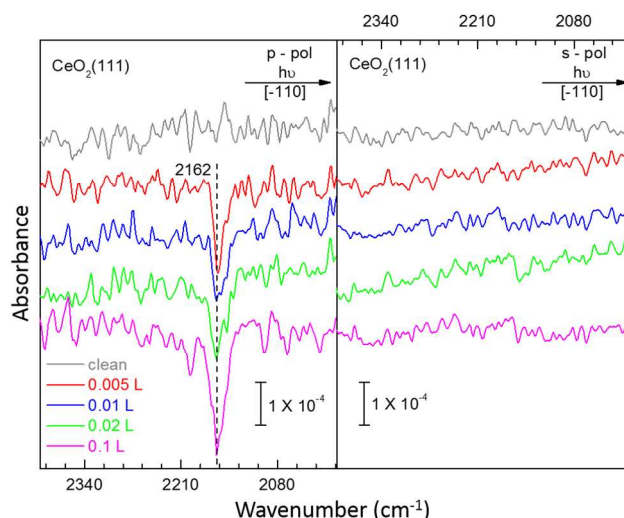spectively (see Fig. S5 to Fig. S9). The blue shift of around 10 cm^{-1} in the

Fig. 3. Experimental IRRA spectra of different doses of CO at 74 K on reduced CeO_2(111) at a grazing incidence angle of 80° with (left) *p*- and (right) *s*-polarized light incident along [-110].

stretch frequency of the CO bound to the defect-induced surface is unusually small, on the basis of previous assignments one would have expected shifts of up to 50 cm^{-1}. In addition, it is surprising to observe a blue-shift for CO bound to a defective site, as on other oxides like TiO_2 the increased binding energy at defect sites (which is also observe here) gives rise to a red-shift. In order to better understand the origins of this unexpected behavior and to assign the defect-induced band, we have carried out first-principle density functional theory (DFT) calculations (see table 1, for details of the calculations see the SI). The results of the calculation allow to assign the defect-induced ν_1 to CO adsorbed at 6-fold coordinated Ce^{4+} ions in the direct vicinity of the vacancy (site 1 in Fig. 1). An assignment to 7-fold coordinated Ce^{3+} ions further away from the vacancy (site 2 in Fig. 1) can be ruled out.

The calculated vibrational frequency of CO bound to the 7-fold coordinated Ce^{4+} on the stoichiometric surface amounts to 2145.2 cm^{-1}, which differs by ~9 cm^{-1} from the experimentally observed frequency of 2154 cm^{-1}. It can clearly be seen from Table 1 that the vibrational frequencies of CO adsorbed on

Table 1. Calculated vibration frequencies V and adsorption energies E_b of CO at various sites on the stoichiometric and reduced CeO2(111) surface (one top-surface oxygen vacancy per supercell, experimental frequencies are listed for comparison).

Substrate	Adsorption Site	DFT ν/cm^{-1} (E_b/eV)	Exp. [cm^{-1}]
	Free molecule	2122.5	2143.5
Ideal	Ce^{4+}	2145.2 (0.28)	2154
Reduced ($O_V$surf)	Ce^{4+} at OV (site 1)	2157.2 (0.40)	2163
	Ce^{4+} (3-fold site V_O)	2169.6 (0.39)	
	Ce^{3+} (site 2)	2150.9 (0.27)	
	Ce^{4+} (site 3)	2143.1 (0.34)	

The calculated frequencies for adsorbed CO were corrected by multiplying the calculated values by a factor of 2143/2122.5 or 1.0097, corresponding to the ratio of the experimental and calculated values for gas-phase CO.
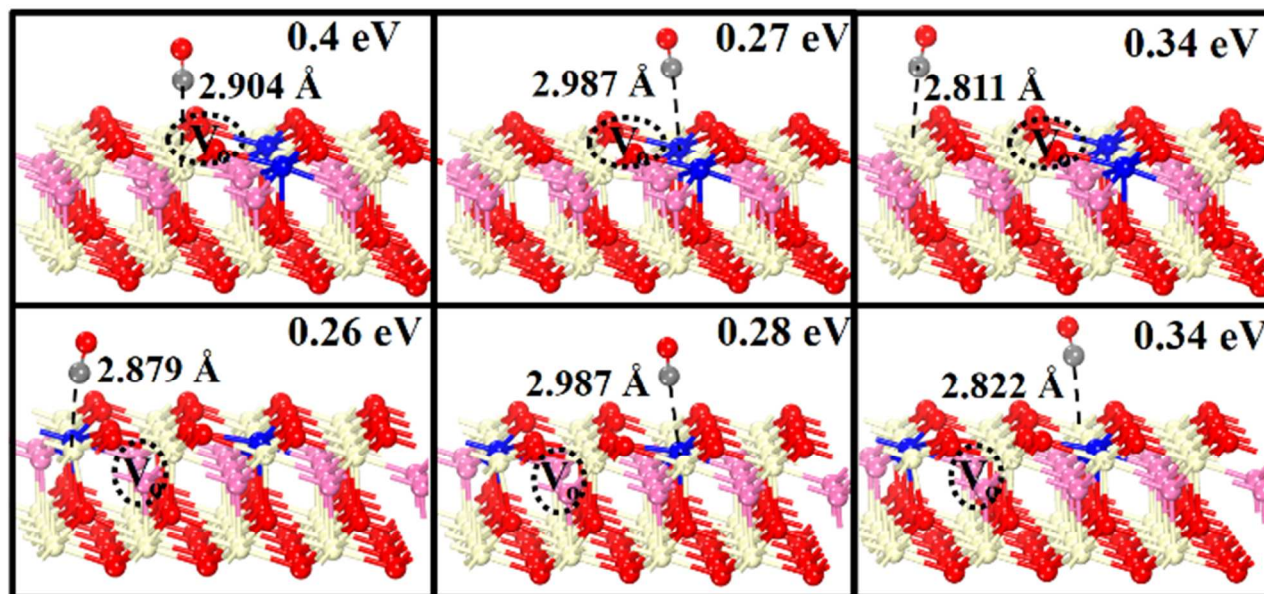

Fig. 4. Calculated structures (side view) of CO adsorbed at different sites on the reduced CeO_2(111) with (a-c) top- and (d-f) sub-surface O vacancy. The calculated OC-Ce distances and adsorption energies are also presented. C atoms are in grey.

defective surface sites shift to higher values, especially for CO adsorbed in a configuration allowing for direct interaction with the vacancy (site 1 in Fig. 1 or center of V_O).

These calculations beautifully corroborate our above assignment, namely that the blue-shift of 10 cm^{-1} seen in the experiment when going from the stoichiometric to the reduced substrate has to be assigned to CO bound to Ce^{4+}-sites in direct vicinity of the vacancy.

Calculations carried out for different CO-coverages (see SI), which in previous work[39,40] has been found to affect both CO binding energies and stretch frequencies, revealed that the local CO concentrations have almost no effect on the CO binding energies. Since in previous assignments of IR-powder data a number of assignments has been reported for CO bound to a 6-fold coordinated Ce^{3+} (present only in a less stable defective surface configuration with the two excess electrons localized at nearest-neighbor Ce cations),[11] we also considered this adsorption site. The adsorption energy was found to be 0.32 eV, i.e. lower compared to 6-fold coordinated Ce^{4+} (cf. Fig. 4a). However, this adsorption energy is slightly larger with respect to that on the 7-fold coordinated Ce^{3+} (cf. Fig. 4b).

CONCLUSIONS

Our experimental and theoretical observations provide a solid basis for the identification of stretch frequencies for CO bound to CeO_2(111) substrates. For CO bound to 7-fold coordinated (i.e., fully coordinated for a surface cation) Ce^{4+}-cations (denoted Ce^{4+}_{7c} where c stands for "coordinated") within the stoichiometric surface, the stretch frequency, ν_1, amounts to 2154 cm^{-1}. The calculated adsorption energy of 0.28 eV for this species is in good agreement with the activa-

tion energy for desorption of 0.27 eV extracted from the temperature programmed desorption experiment.

Surprisingly, the CO species bound to defective parts of the surface exhibits a blue-shift (in contrast to other oxides). For Ce-ions in direct vicinity of the oxygen-vacancy, the corresponding blue-shift amounts to 10 cm^{-1}. We tentatively ascribe the increased adsorption energy and higher vibrational frequency observed for this species to electrostatic interactions resulting from a coupling of the CO dipole and the dipole of the top-surface-O-Ce double layer when the molecule moves inside the vacancy.

Based on the best agreement in the stretch frequency, we assign the band at 2163 cm^{-1} to CO at Ce^{4+} ions at the O_V site. Note also that the number of available Ce^{4+}_{6c}-sites is three times larger than that of the 3-fold hollow sites inside the vacancy. In fact, the spectra displayed in Fig. 3b would be consistent with the presence of a weak feature at higher frequencies, where theory would predict the position of the stretch frequency for CO adsorbed within the O-vacancies. As the calculated binding energy is very similar to the one calculated for adsorption on Ce^{4+} ions at the vacancy, one would expect that this site would be populated as well. Our results demonstrate that the coordination geometry can play a decisive role for weak chemical interactions on oxide surfaces. While on TiO_2 and many other oxides the frequency of adsorbed CO is mainly given by the charge state of the metal cation, the coordination geometry exhibits a more pronounced influence for CeO_2.

ASSOCIATED CONTENT

Supporting Information

Computational details, CO stretch frequency assignment for ceria powder, IR spectra of CO adsorbed on stoichiometric

and reduced CeO$_2$ with light incident along the [-211] direction, XPS data including analysis of the vacancy concentration on the stoichiometric and reduced surface, IRRAS desorption experiment on the stoichiometric and reduced surface (including determination of the activation energy of desorption). This material is available free of charge via the Internet at http://pubs.acs.org.

AUTHOR INFORMATION

Corresponding Authors:

christof.woell@kit.edu
xgong@ecust.edu.cn

Notes

The authors declare no competing financial interests.

ACKNOWLEDGMENT

REFERENCES

(1)   Paier, J.; Penschke, C.; Sauer, J. Chemical reviews 2013, 113, 3949.

(2)   Idriss, H.; Scott, M.; Llorca, J.; Chan, S. C.; Chiu, W.; Sheng, P.-Y.; Yee, A.; Blackford, M. A.; Pas, S. J.; Hill, A. J.; Alamgir, F. M.; Rettew, R.; Petersburg, C.; Senanayake, S. D.; Barteau, M. A. ChemSusChem 2008, 1, 905.

(3)   Wang, X.; Rodriguez, J. A.; Hanson, J. C.; Gamarra, D.; Martínez-Arias, A.; Fernández-García, M. The Journal of Physical Chemistry B 2005, 110, 428.

(4)   Xu, W.; Si, R.; Senanayake, S. D.; Llorca, J.; Idriss, H.; Stacchiola, D.; Hanson, J. C.; Rodriguez, J. A. Journal of Catalysis 2012, 291, 117.

(5)   Rodriguez, J. A.; Liu, P.; Hrbek, J.; Evans, J.; Pérez, M. Angewandte Chemie International Edition 2007, 46, 1329.

(6)   Idriss, H.; AL-SHANKITI, I.; Choi, Y. M.; Al-Otaibi, F. M.; WO2014016790-A1: 2014.

(7)   Al-Shankiti, I.; Al-Otaibi, F.; Al-Salik, Y.; Idriss, H. Top Catal 2013, 56, 1129.

(8)   Chueh, W. C.; Falter, C.; Abbott, M.; Scipio, D.; Furler, P.; Haile, S. M.; Steinfeld, A. Science 2010, 330, 1797.

(9)   Furler, P.; Scheffe, J. R.; Steinfeld, A. Energy & Environmental Science 2012, 5, 6098.

(10)   Ganduglia-Pirovano, M. V.; Da Silva, J. L. F.; Sauer, J. Physical Review Letters 2009, 102, 026101.

(11)   Li, H.-Y.; Wang, H.-F.; Gong, X.-Q.; Guo, Y.-L.; Guo, Y.; Lu, G.; Hu, P. Physical Review B 2009, 79.

(12)   Shoko, E.; Smith, M. F.; Ross, H. M. Journal of Physics: Condensed Matter 2010, 22, 223201.

(13)   Jerratsch, J.-F.; Shao, X.; Nilius, N.; Freund, H.-J.; Popa, C.; Ganduglia-Pirovano, M. V.; Burow, A. M.; Sauer, J. Physical Review Letters 2011, 106, 246801.

(14)   Wang, Y.-G.; Mei, D.; Li, J.; Rousseau, R. The Journal of Physical Chemistry C 2013, 117, 23082.

(15)   Plata, J. J.; Márquez, A. M.; Sanz, J. F. The Journal of Physical Chemistry C 2013, 117, 25497.

(16)   Farra, R.; Wrabetz, S.; Schuster, M. E.; Stotz, E.; Hamilton, N. G.; Amrute, A. P.; Perez-Ramirez, J.; Lopez, N.; Teschner, D. Physical chemistry chemical physics : PCCP 2013, 15, 3454.

(17)   Bazin, P.; Saur, O.; Lavalley, J. C.; Daturi, M.; Blanchard, G. Physical Chemistry Chemical Physics 2005, 7, 187.

(18)   Tabakova, T.; Boccuzzi, F.; Manzoli, M.; Andreeva, D. Applied Catalysis A: General 2003, 252, 385.

(19)   Daturi, M.; Binet, C.; Lavalley, J.-C.; Galtayries, A.; Sporken, R. Physical Chemistry Chemical Physics 1999, 1, 5717.

(20)   Binet, C.; Daturi, M.; Lavalley, J.-C. Catalysis Today 1999, 50, 207.

(21)   Mekhemer, G. A. H.; Zaki, M. I. Adsorption Science & Technology 1997, 15, 377.

(22)   Badri, A.; Binet, C.; Lavalley, J.-C. Journal of the Chemical Society, Faraday Transactions 1996, 92, 1603.

(23)   Zaki, M. I.; Vielhaber, B.; Knoezinger, H. The Journal of Physical Chemistry 1986, 90, 3176.

(24)   Bozon-Verduraz, F.; Bensalem, A. Journal of the Chemical Society, Faraday Transactions 1994, 90, 653.

(25)   Li, C.; Sakata, Y.; Arai, T.; Domen, K.; Maruya, K.-i.; Onishi, T. Journal of the Chemical Society, Faraday Transactions 1: Physical Chemistry in Condensed Phases 1989, 85, 929.

(26)   St Petkov, P.; Vayssilov, G. N.; Liu, J.; Shekhah, O.; Wang, Y.; Wöll, C.; Heine, T. Chemphyschem : a European journal of chemical physics and physical chemistry 2012, 13, 2025.

(27)   Mudiyanselage, K.; Kim, H. Y.; Senanayake, S. D.; Baber, A. E.; Liu, P.; Stacchiola, D. Physical chemistry chemical physics : PCCP 2013, 15, 15856.

(28)   Xu, M.; Noei, H.; Fink, K.; Muhler, M.; Wang, Y.; Wöll, C. Angewandte Chemie 2012, 51, 4731.

(29)   Buchholz, M.; Weidler, P. G.; Bebensee, F.; Nefedov, A.; Wöll, C. Physical Chemistry Chemical Physics 2014, 16, 1672.

(30)   Kresse, G.; Hafner, J. Physical Review B 1993, 47, 558.

(31)   Kresse, G.; Hafner, J. Physical Review B 1994, 49, 14251.

(32)   Perdew, J. P.; Burke, K.; Ernzerhof, M. Physical Review Letters 1996, 77, 3865.

(33)   Perdew, J. P.; Burke, K.; Ernzerhof, M. Physical Review Letters 1997, 78, 1396.

(34)   Blöchl, P. E. Physical Review B 1994, 50, 17953.

(35)   Kresse, G.; Joubert, D. Physical Review B 1999, 59, 1758.

(36)   Guss, P.; Foster, M. E.; Wong, B. M.; Doty, F. P.; Shah, K.; Squillante, M. R.; Shirwadkar, U.; Hawrami, R.; Tower, J.; Yuan, D. J Appl Phys 2014, 115.

(37)   Song, Y. L.; Yin, L. L.; Zhang, J.; Hu, P.; Gong, X. Q.; Lu, G. Z. Surface Science 2013, 618, 140.

(38)   Xu, M.; Gao, Y.; Moreno, E. M.; Kunst, M.; Muhler, M.; Wang, Y.; Idriss, H.; Wöll, C. Physical Review Letters 2011, 106.

(39)   Rohmann, C.; Metson, J. B.; Idriss, H. Surface Science 2011, 605, 1694.

(40)   Rohmann, C.; Metson, J. B.; Idriss, H. Physical chemistry chemical physics : PCCP 2014, 16, 14287.